8A.1

THE VERTICAL STRUCTURE OF THE HAPPY, TEXAS TORNADO OF 5 MAY 2002: MOBILE, W-BAND, DOPPLER-RADAR OBSERVATIONS

Howard B. Bluestein* and Christopher C. Weiss
University of Oklahoma
Norman, Oklahoma

Andrew L. Pazmany
University of Massachusetts
Amherst, Massachusetts

1. INTRODUCTION

Where the highest horizontal-wind speeds are in tornadoes is of great interest to both theoreticians and structural engineers. Experiments with laboratory models (e.g., Church et al. 1979) and, most recently, with large-eddy simulations of tornado-like vortices (e.g., Lewellen et al. 2000), have shown how the character of the flow (i.e., radial and vertical profiles of the vertical and horizontal wind) depends upon the swirl ratio. Verification of these results based on observations of real tornadoes, however, has been relatively lacking. Wakimoto and Martner (1992), using two fixed-site X-band radars whose antennas had a 0.8° beamwidth, and Wurman and Gill (2000), using a mobile X-band Doppler radar whose antenna had a 1.2° beamwidth, produced vertical cross sections of Doppler velocity and radar reflectivity through a landspout in Colorado and a supercell tornado in West Texas, respectively, by synthesizing data collected in scans at constant elevation angle.

Resolving air motions as close to the ground as possible requires a very narrow beam and a relatively weak sidelobe pattern. To achieve even higher spatial resolution, a W-band (3-mm wavelength) truck-mounted pulsed Doppler radar system has been used to probe tornadoes in the southern Plains (Bluestein and Pazmany 2000). The antenna of this radar system has a half-power beamwidth of only 0.18°; the radar has range gates every 15 m for pulses whose length are also 15 m, and employs polarization diversity pulse-pair processing (PDPP) (Pazmany et al. 1999) to achieve a very high maximum unambiguous Doppler velocity (±79 m s^{-1}).

The purpose of this paper is to describe a dataset collected by the W-band radar in a tornado near Happy, TX on 5 May 2002, in which a number of RHIs were collected below cloud base and near the ground through the tornado vortex.

2. NATURE OF THE DATA COLLECTED

Data were collected beginning when the tornado, which was mature, was passing through and east of Happy, TX, located 7.2 km to the west-southwest of the radar. The tornado inflicted "extensive" damage (SPC website) as it moved through the town at about 1945 CDT (all times given in CDT) and continued east-northeastward toward the radar (Fig. 1). Several homes were destroyed, a roof was blown off a church; three people were killed and four were injured.

* Corresponding author address: Howard B. Bluestein, School of Meteorology, Univ. of Oklahoma,Norman,OK 73019; e-mail: hblue@ou.edu

Figure 1. Tornado to the west-southwest of the W-band radar seen in the foreground along with the first author, at approximately 1949 CDT, 5 May 2002, 7.2 km east of Happy, TX. Photograph courtesy of M. Kramar.

Low-elevation-angle sector scans (just above the ground) were collected first while the tornado was at 6.2 – 4.4 km range. Then a series of RHIs on the right sight, left side, and through the center of the tornado were collected while the tornado was at 3.1 - 1.6 km range; at these ranges the azimuthal resolution was 10 - 20 m. So, the pulse volume when the RHIs were taken was about 15 m X 15 m X 15 m. Each scan was accompanied by boresighted video so that the locations with respect to the visible condensation funnel and debris cloud could be determined. From the boresighted video, it was determined that the radar platform was tilted approximately 5° to the right, or toward the north. Finally, more low-elevation-angle sector scans were collected as the tornado reached 1.1 km in range while it was dissipating. It was fortunate that the RHIs were collected when the range was within 3.1 km: Prior to then, attenuation seriously limited the intensity of the backscatter from the tornado (Fig. 2) and after then the tornado was too close (within 1.5 km) to do PDPP processing, so that only conventional pulse-pair processing was usable and the maximum unambiguous Doppler velocity, which was only ±8 m s^{-1}, made unfolding aliased data difficult, if not impossible.

As a result of a software problem, relative azimuth (in the constant elevation-angle sector scans) and elevation angles (in the RHIs) were not recorded. The azimuth and elevation angles were restored to the data record from each beam after viewing the boresighted video and from the known scan rates. Data collected while the antenna was not scanning and/or pointed at or below the ground level and/or at the top of each scan, were not included. It is therefore possible that some RHIs are shifted slightly when the ground is not exactly at 0° elevation angle.

The dimensions of the condensation funnel of the tornado and that of its surface debris cloud were determined by photogrammetrically analyzing medium-format (70 mm) transparencies taken by the first author. The distance to the visual features was estimated from the radar data.

3. RESULTS

a. PPIs

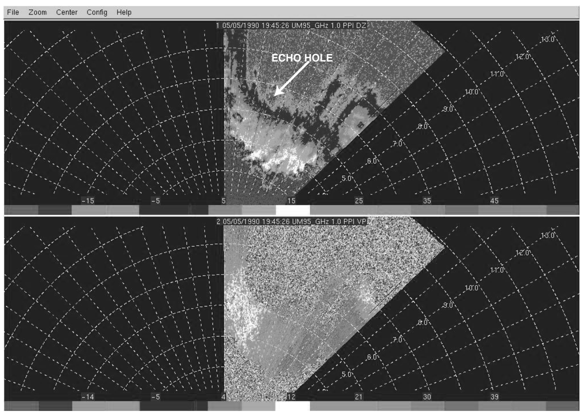

Figure 2. PPI of radar reflectivity in dBZe (top) and ground-relative Doppler (PDPP) velocity in m s^{-1} (bottom) at 1945:26 CDT. Range rings every 1 km; relative-azimuth rays every 5°. Echo hole associated with the tornado at 5.5 km range is severely attenuated.

The tornado (marked by a 300-m wide echo hole and a cyclonic-shear signature) was located behind an arc of relatively high reflectivity. The radar scan cut a quasi-horizontal path just above the debris cloud, whose top, from photogrammetric analysis, was found to be about 180-200 m AGL. Unfortunately, since the radar platform was tilted slightly, the surface layer in the tornado was not sampled. However, to the north of the tornado (in the far right of Fig. 2), air motion of 50 m s^{-1} away from the radar was found below 50 m AGL, in an area where scud-cloud tags were seen, on the boresighted video, moving rapidly toward the tornado.

While the PDPP velocity data are too noisy to use in the area of and that flanking the echo hole, ordinary pulse-pair velocity data are of high quality and unfolding the data is pending: It was not possible to determine the core radius, and other tornado parameters based on the PDPP data, but should be possible later after the ordinary pulse-pair data have been corrected.

From the series of PPIs, it was determined that the component of motion of the tornado along the line-of-sight of the radar was about 13 m s^{-1}, toward the radar (i.e., from west to east). It was not possible to determine the component of motion normal to the line-of-sight because the azimuth positions in each scan are known only in a relative sense. However, in a qualitative sense, the motion was from left to right, so that the component of motion normal to the line-of-sight was to the north, and less in magnitude than that of the along-the-line-of-sight component.

b. RHIs

The high-resolution RHIs are the unique aspect of the Happy, TX dataset. A few representative vertical cross sections of radar reflectivity and Doppler velocity are shown below (Figs. 4 and 6), along with schematic illustrations showing the relationship between the scans, the condensation funnel, and the ground (Figs. 3 and 5).

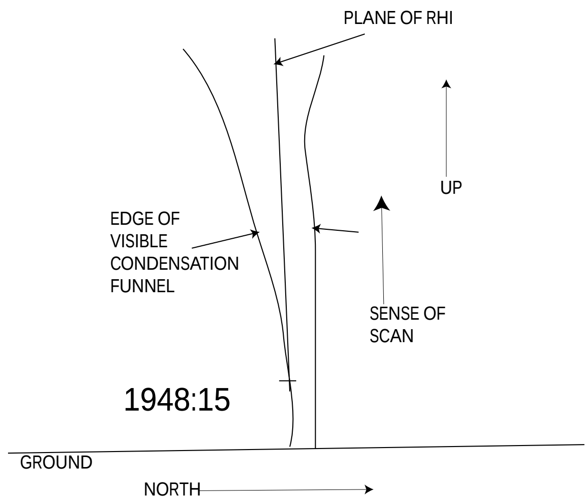

Figure 3. Schematic illustrating relationship between RHI scan and edges of the visible condensation funnel at 1948:15 CDT.

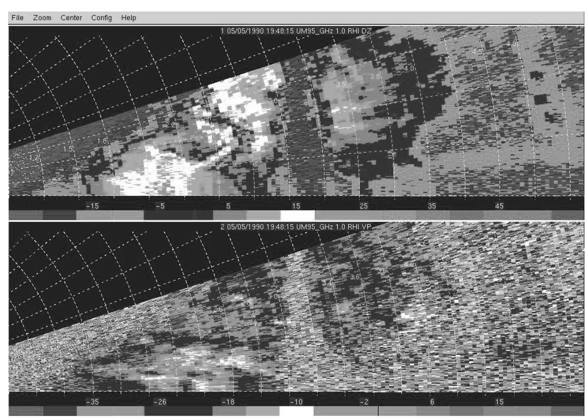

Figure 4. RHI of radar reflectivity in dBZe (top) and ground-relative Doppler (PDPP) velocity in m s^{-1} at 1948:15 CDT. The sign of the Doppler velocities in this and other RHI panels is the reverse of meteorological convention: Approaching (receding) velocities are denoted by positive (negative) wind speeds. Center of the tornado is marked by the vertically oriented echo hole at 3.1 km range. Range rings every 250 m; relative-azimuth rays every 5°.

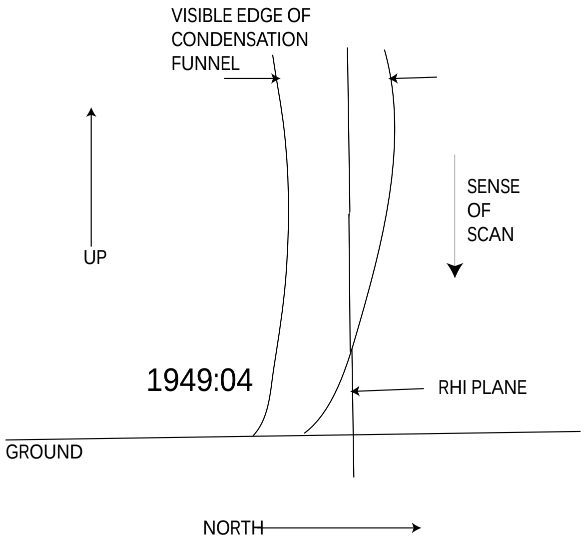

Figure 5. As in Fig. 3, but at 1949:02 CDT.

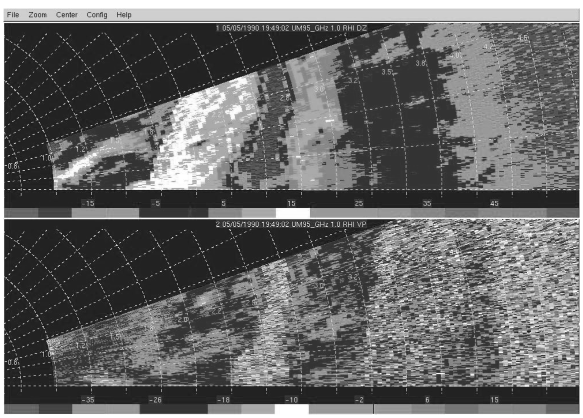

Figure 6. As in Fig. 4, but at 1949:02 CDT. Center of the tornado is marked by the slightly tilted echo hole at about 2.5 km range. (Some of the tilt may be an artifact of the 30 s needed to complete the RHI sweep and the motion of the tornado toward the radar.)

To interpret the RHIs properly, it is necessary to relate the edges of the tornado's condensation funnel to the characteristics of the tornado vortex. From photogrammetric analysis, it was determined that the width of the condensation funnel at cloud base was approximately 70-75 m (uncertainties are due mainly to uncertainties in the distance to the features); the width of the debris cloud at the ground was 250-275 m; the vertical depth of the debris cloud was 180-200 m; the height of cloud base at the tornado was 500-550 m AGL. In some instances the RHI cut from one side of the tornado through the center as a result of the tilt of the tornado vortex with height and the tilt of the radar platform.

Since the core radius of the tornado is yet to be determined, a comparison between the width of the condensation funnel and the debris cloud with the width of the tornado core is not available. However, it is suspected that the width of the condensation funnel is less than the width of the core because the latter is so narrow (cf., e.g., Bluestein et al. 2003).

In all RHIs the center of the tornado, above the debris cloud, was marked by a vertically oriented echo-free hole about 160 m in diameter and one about 300 m in diameter within the debris cloud. The echo-free hole was widest around 100 m AGL, and extended down to within about 60 m of the ground.

Another ubiquitous feature seen in the RHIs of the reflectivity field when the far left portion of the field was not cut off was an arc of enhanced reflectivity seen to the left in the images (i.e., in front of the tornado), extending from the ground up to about 300 m AGL. Below this arc, there was vertical shear in the Doppler velocity consistent with a vertical circulation into the plane of the figure in a clockwise sense.

Since most of the RHIs were made near the edges of or within the visible condensation funnel, it is likely that most of them did not sample the very high wind speeds associated with the core. Efforts to relate the Doppler velocity field to the tornado's azimuthal wind component in the core were therefore not generally successful. However, maximum approaching Doppler velocities were found in RHIs taken to the left of the condensation funnel at 1948:29 and 1950:12 (not shown); maximum receding Doppler velocities were found in the RHI taken along the right edge of the condensation funnel at 1948:53 (not shown); no RHIs were taken to the right of the condensation funnel.

Maximum Doppler velocities at and before 1949:35 were in general found around 300 m AGL. The reader is reminded that 13 m s^{-1} must be added to the Doppler velocity field to find the tornado-relative wind field. Better (in color) and more documentation will be presented at the conference.

At 1948:44, the core of the tornado was sampled inadvertently while the antenna was being repositioned between successive RHIs. In this "scan," the antenna motion was intermittent, thus precluding a regular sector-scan image. However, as the antenna moved across the tornado near the ground, maximum Doppler velocities of 60 m s^{-1} in the approaching direction, to the left side of the tornado, and 20 m s^{-1} in the receding direction, to the right side of the tornado, were noted.

3. SUMMARY AND CONCLUSIONS

The Happy, TX dataset was the first one in which we collected RHI data through a tornado. A summary of the reflectivity structure is shown in Fig. 7. The reflectivity structure is similar in a few respects to that found by Wurman and Gill (2000). In each, the hole does not extend all the way down to the ground; also, the diameters of the echo-free eyes are similar.

A different feature of the Happy, TX eye is its broadening out just above the ground; it is widest at 100 m AGL. It is hypothesized that this broadening may be due to centrifuging of scatterers radially outward near or just within the tornado core and to the tornado's secondary circulation. Dowell (2003, personal communication) has numerically simulated tornadolike vortices having particles of various sizes injected into it. Such a study could explain more quantitatively the observed shape of the eye's reflectivity profile.

The height AGL at which the maximum azimuthal wind speeds in tornadoes is found varies with the swirl ratio and the nature of the boundary conditions (Lewellen et al. 2000). It was surprising that the highest wind speeds were found so high, around 300 m AGL. The result could have been different, however, if the core had actually been sampled. In addition, the effects of turbulence and the transient nature of the tornado vortex should be accounted for by sampling as often as possible.

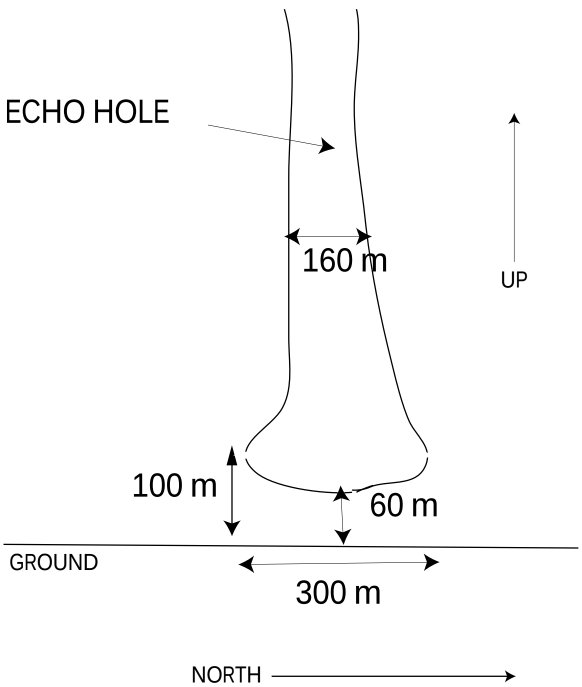

Figure 7. Model of the radar-reflectivity distribution in the Happy, TX tornado. Figure is not drawn to scale.

In the case of the Happy, TX tornado, the motion of the tornado had a significant component along the line-of-sight of the radar. It would be better for data collection if the tornado moved largely across the line of sight, so that RHIs could be taken at a fixed location; then, as the tornado translated by the plane scanned in the RHI, the spatial resolution across the tornado would be maximized, and its core could be sampled.

In addition, since the core of the tornado likely lies outside the visible edge of the condensation funnel (e.g., Bluestein et al. 2003), RHIs should begin well to the side of the condensation funnel. Furthermore, there is some evidence that debris clouds at the surface in intense vortices can be narrower than the core diameter (Bluestein et al. 2003; Bluestein et al. 2004). It is thus concluded that RHI scans should begin outside the edge of the debris cloud also and that the tornado should then pass through the RHI plane until the opposite edge of the debris cloud has passed. Efforts to minimize the effects of tilting of the RHI plane should be undertaken by more carefully leveling the radar platform.

Knowledge of the core diameter of the tornado being sampled is very important. If attenuation makes it difficult to determine the core diameter when using sector scans, then it may be necessary to increase the pulse length of the radar to enhance the sensitivity at the expense of along-the-line-of-sight spatial resolution.

A final improvement in the W-band operations is suggested: The scanning of the radar antenna is controlled by the operator, who watches the monitor of the boresighted video camera. It would be helpful if the video image were better exposed by allowing the operator to manually adjust the aperture of the camera lens. In the current configuration, the tornado condensation funnel is usually overexposed when the antenna is pointed at low elevation angle, because the camera's automatic exposure system is contaminated by the darker ground.

ACKNOWLEDGMENTS

This research was funded by NSF grants ATM-9912097 at OU and ATM-9616730 at U. Mass. Support was also provided by the School of Meteorology at the University of Oklahoma (OU). The second author operated the radar in the field. Brendan Fennell also participated in this field project.

REFERENCES

Bluestein, H. B., C. C. Weiss, and A. L. Pazmany, 2004: Doppler-radar observations of dust devils in Texas. Mon. Wea. Rev. (in review)

Bluestein, H. B., W.-C. Lee, M. Bell, C. C. Weiss, and A. L. Pazmany, 2003: Mobile-Doppler-radar observations of a tornado in a supercell near Bassett, Nebraska on 5 June 1999. Part II: Tornado-vortex structure. Mon. Wea. Rev. (in review)

Bluestein, H., and A. L. Pazmany, 2000: Observations of tornadoes and other convective phenomena with a mobile, 3-mm wavelength, Doppler radar: The spring 1999 field experiment. Bull. Amer. Meteor. Soc., **81**, 2939-2951.

Church, C. R., J. T. Snow, G. L. Baker, and E. M. Agee, 1979: Characteristics of tornado-like vortices as a function of swirl ratio: A laboratory investigation. J. Atmos. Sci., **36**, 1755-1776.

Lewellen, D. C., W. S. Lewellen, and J. Xia, 2000: The influence of a local swirl ratio on tornado intensification near the surface. J. Atmos. Sci., **57**, 527-544.

Pazmany, A. L., J. C. Galloway, J. B. Mead, I. Popstefanija, R. E. McIntosh, and H. B. Bluestein, 1999: Polarization diversity pulse pair technique for millimeter-wave Doppler radar measurements of severe-storm features. J. Atmos. Ocean. Tech., **16**, 1900-1911.

Wakimoto, R. M., and B. E. Martner, 1992: Observations of a Colorado tornado. Part II: Combined photogrammetric and Doppler radar analysis. Mon. Wea. Rev., **120**, 522-543.

Wurman, J., and S. Gill, 2000: Finescale radar observations of the Dimmitt, Texas (2 June 1995), tornado. Mon. Wea. Rev., **128**, 2135-2164.